UNLIMITED SAMPLING WITH SPARSE OUTLIERS: EXPERIMENTS WITH IMPULSIVE AND JUMP OR RESET NOISE

Ayush Bhandari

Dept. of Electrical and Electronic Engg., Imperial College London, SW72AZ, UK.
Email: `a.bhandari@imperial.ac.uk` or `ayush@alum.mit.edu`

ABSTRACT

Unlimited Sensing is a sampling protocol that recovers high dynamic range input signals from their low dynamic range, modulo samples. Bridging the gap between theory and practice, recently, a hardware validation of the unlimited sampling method was presented. Taking another step in this direction, in this paper, we study the problem of recovery from modulo samples contaminated by sparse outliers (noise). Our hardware experiments suggest that impulsive and jump or reset noise can be sources of sparse outliers in the measurements. Such a noise model has not been considered in literature and can lead to the breakdown of the conventional recovery methods. To overcome this problem, we present a mathematically guaranteed algorithm that is based on spectral estimation. Our method perfectly recovers the signal (up to a constant) when the sampling criterion is met and no other noise sources are present. In real experiments where quantization and system noise (*e.g.* additive Gaussian) play a role, our approach offers a competitive performance. Hardware experiments with our modulo ADC validate the practical utility of our method.

Index Terms— ADC, modulo, non-linear reconstruction, sampling, Prony's method, super-resolution.

1. INTRODUCTION

Digital acquisition of signals is the stepping stone of almost all modern world applications. Its roots trace back to Shannon's pioneering work on sampling theory which is implemented in practice using analog-to-digital converters (ADCs). Point-wise sampling is a mature technology and its many advances have been made possible not only by studying theoretical underpinnings of sampling theory but also by developing strategies to counter distortions arising in practice; typically attributed to system noise and quantization. Beyond these distortions, a fundamental bottleneck that arises in practice is the dynamic range (DR) of the ADC. For ADC based digital acquisition to work, the DR of the ADC should be matched to the signal of interest. If this aspect is ignored, the resulting measurements will be saturated or clipped, thus resulting in permanent information loss. Since traditional signal processing pipeline assumes no control over acquisition protocol, typically the task of matching the DR of the ADC to the signal of interest is left to the hardware engineers. In cases where measurements are clipped, signal processing engineers resort to numerical techniques for recovering data or parameter estimation, cf. [1–5]. However, the algorithms can only go so far when the measurements entail a permanent loss of information. This barrier (of clipping) may pose severe limitations in applications such as biomedical engineering where vital signals have health implications and space exploration [6] where experiments are a one-time opportunity and exceedingly expensive.

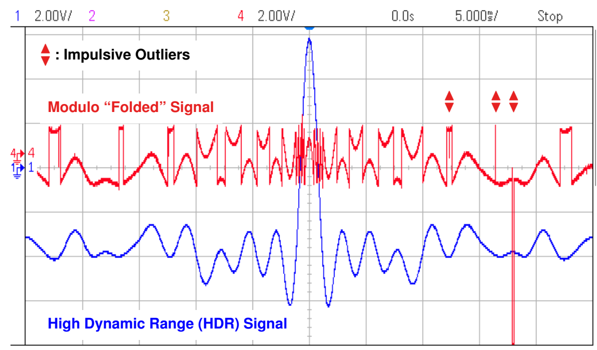

(a) Example of *impulse* noise. In this case, impulse-like outliers contaminate the signal at arbitrary locations.

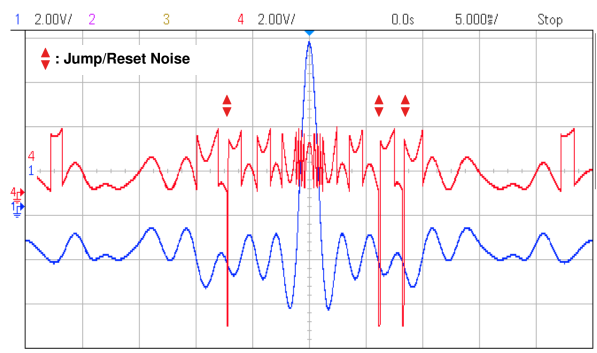

(b) Example of *jump* or *reset* noise. In this case, outliers occur at the instants when signal folding is triggered.

Fig. 1: Oscilloscope screenshot showing sparse outliers at the output of our modulo ADC implementing the unlimited sampling strategy.

A Computational Sampling Approach. Taking an alternative route to the DR bottleneck in digital systems, in recent years, we have been developing the *Unlimited Sensing Framework* (USF) [7–10]. Beyond the traditional paradigm—*capture first, process later*—the USF capitalizes on a joint design of hardware and algorithms to bridge the gap between the theory and practical implementation of conventional sampling framework. In doing so, the clipping problem can be eliminated. More concretely,

- in *hardware*, we implement signal folding by injecting modulo non-linearity. Thus, amplitudes exceeding the ADC's DR are folded in. In our upcoming work [10], we have built a mod-

Ayush Bhandari's work is supported by the UK Research and Innovation council's FLF Program “Sensing Beyond Barriers” (MRC Fellowship award no. MR/S034897/1). Further details on Unlimited Sensing and upcoming materials on *reproducible research* are available via `https://bit.ly/USF-Link`.

ulo ADC—the US-ADC. Interested readers are invited to see the US-ADC in action at `https://youtu.be/prV40WlzHh4`. US-ADC output is also shown in Fig. 1, but the signal is corrupted with *sparse outliers*; the topic of discussion in this paper.

- in the *recovery* phase, reconstruction of original signal is enabled by mathematical algorithms. For bandlimited functions, we have shown that constant factor oversampling (independent of λ) guarantees recovery [7]. A similar principle holds for *quantized* modulo samples [8]. When working with real experiments, we provide examples of reconstruction in [10, 11] as well as in our upcoming paper [12].

In essence, the USF enables *high dynamic range* (HDR) signal recovery from its *low dynamic range* (LDR), modulo samples. Beyond sampling theory and acquisition protocols [13, 14], this principle also applies to fundamental signal processing topics such as sensor array processing [15,16], sparse signal recovery [17,18] and computational imaging, *e.g.* HDR imaging [19] and tomography [20,21].

Motivation. This paper is motivated by challenges that arise from an end-to-end implementation of the USF. In the course of developing and refining the hardware testbed for the USF, we have *experimentally* observed that in certain scenarios, sparse outliers can contaminate the modulo samples. Such outliers can be broadly classified into,

- **Impulsive or Shot Noise (I/S-N)** As shown in the oscilloscope screen view in Fig. 1(a), I/S-N manifests as an erratic spike sequence in the modulo data. The I/S-N model has been widely studied in a variety of contexts [22–24] and shows up as electronic interference in hardware, among other scenarios.
- **Jump or Reset Noise (J/R-N)** As shown in in Fig. 1(b), the J/R-N shows up as "spiky" jumps at the instant of folding, hence the reference to *jump* or *reset* noise. We attribute these jumps to instabilities associated with electronic components used in the printed circuit board (PCB). Unlike the case of I/S-N, we note that the jump amplitude of J/R-N is more or less within the same range.

Such contaminations can lead to a breakdown of the recovery algorithms unless appropriate reconstruction strategies are devised for combating the effect of sparse outliers, namely, I/S-N and J/R-N. This motivates computational approaches that can recover HDR signals from corrupted, modulo samples, as shown in Fig. 1.

Contributions. To our knowledge, recovery from sparse outliers has not be considered in the context of modulo sampling. The goal of this paper is to (a) model (phenomenologically) the sparse outliers based on experiments, (b) develop a HDR recovery method that is agnostic to λ (inspired by [10]). This leads to a *one-shot inversion* approach; rather than first denoising modulo samples followed by reconstruction [7, 8, 25], and (c) validate our method on real experiments based on the US-ADC. The take-home message of this work is as follows;

- ► Provided that the I/S-N or J/R-N density is lower than the sampling density of modulo samples, *exact recovery* is guaranteed when no other sources of noise are present.
- ► When working with hardware, additional noise sources may be present *e.g.* quantization and Gaussian noise. Our reconstruction algorithm offers a competitive performance that is empirically robust; this is validated via hardware experiments in Section 4.

By developing theoretical models that are validated via experiments, our end-to-end work brings the USF closer to practice.

Related Research Efforts and Context. USF and modulo sampling in the noisy scenario has been discussed in different research papers [8, 26–30]. Different from the topic of this paper, all of the papers

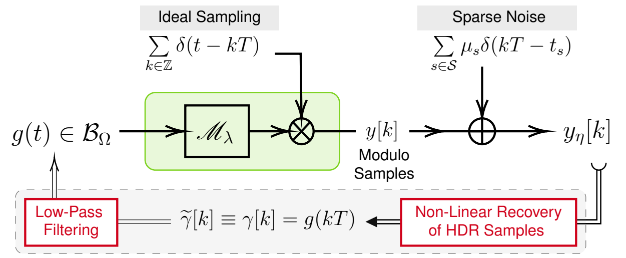

Fig. 2: Unlimited Sampling pipeline, sparse noise model and overview of reconstruction strategy. In the above, δ denotes the Dirac distribution.

known to us discuss the case bounded or Gaussian noise. Additive noise in the pre-modulo regime is focal point of discussion in [26–28,30]. The scenario when modulo samples are corrupted by additive noise is considered in [8, 29]. Mathematical guarantees have been studied for the different cases (a) bounded noise [8], (b) Gaussian noise [30], and (c) combination of both [27, 28].

2. SAMPLING PIPELINE AND PROBLEM SETUP

In this paper, we will be working with square-integrable, Ω–bandlimited functions, $g \in \mathcal{B}_\Omega$, that are τ–periodic or $g(t) = g(t+\tau), \forall t \in \mathbb{R}$. The periodicity of g allows us to work with samples in a finite time window of size τ, which is the case with hardware experiments, and also allows for the Fourier Series representation,

$$g(t) = \sum_{|p|\leqslant P} \widehat{g}_p e^{\jmath p\omega_0 t}, \quad \omega_0 = \frac{2\pi}{\tau}, \quad P = \left\lceil \frac{\Omega}{\omega_0} \right\rceil \tag{1}$$

with Fourier weights $\widehat{g}_p$. Uniform sampling of $g(t) \in [0,\tau)$ with sampling period $T > 0$ results in $\{\gamma[k] = g(kT)\}_{k=0}^{K-1}$. Note that $K \geqslant 2P+1$ completes the linear system in (1) and one can solve for $\widehat{g}_p$. In the oversampled regime, $\widehat{g}_p$ is defined on the set $\mathbb{E}_{P,K} = [0,P] \cup [K-P, K-1]$ and $\widehat{g}_p = 0, p \in ([0, K-1] \setminus \mathbb{E}_{P,K})$ (due to the bandlimitedness assumption).

In the USF, modulo non-linearity is applied in the continuous domain; $g(t)$ is folded using the *centered* modulo operation [7, 8],

$$\mathscr{M}_\lambda : g \mapsto 2\lambda \left(\left[\!\left[\frac{g}{2\lambda} + \frac{1}{2} \right]\!\right] - \frac{1}{2} \right), \quad [\![g]\!] \stackrel{\text{def}}{=} g - \lfloor g \rfloor, \quad \lambda \in \mathbb{R}^+ \tag{2}$$

where $\lfloor g \rfloor = \sup\{k \in \mathbb{Z} | \, k \leqslant g\}$ (floor function). This results in the folded signal $\mathscr{M}_\lambda(g(t))$ shown in Fig. 1 (barring the outliers). The continuous-time folded signal $\mathscr{M}_\lambda(g(t))$ is then uniformly sampled as shown in Fig. 2. This results in modulo samples, $y[k] = \mathscr{M}_\lambda(g(kT))$. In our work, sparse outliers contaminating the modulo samples (cf. Fig. 2) are modeled as a finite sum of spikes and hence,

$$y_\eta[k] = \underbrace{\mathscr{M}_\lambda(g(kT))}_{y[k]} + \eta[k], \quad \eta[k] \stackrel{\text{def}}{=} \underbrace{\sum\nolimits_{s\in\mathcal{S}} \mu_s \delta(kT - t_s)}_{\text{Outliers: I/S-N and J/R-N}} \tag{3}$$

where, i) $\eta[k]$ comprises of $|\mathcal{S}| = S$ Dirac masses (δ) and models the I/S-N or J/R-N or a combination of both, ii) μ_s are the unknown weights, and iii) $t_s \in (T\mathbb{Z}) \cap [0,\tau)$ are the unknown instances. Note that one observes a different realization of $\eta[k]$ depending on the window of observation $[\mathbb{Z}\tau, \mathbb{Z}\tau + \tau)$. This model is based on experiments conducted with the US-ADC and as we shall see in the experiments, this indeed accurately matches the practice.

Goal: Given K noisy measurements $y_\eta[k], k = 0, \ldots, K-1$ of $g \in \mathcal{B}_\Omega$, our goal is to recover the unfolded samples $\gamma[k]$. Once $\gamma[k]$'s are known, $g(t)$ is obtained by low-pass filtering (sinc-interpolation). In this paper, we are primarily interested in addressing the following two questions related to our goal. Q_1) What sampling density guarantees recovery of γ from y_η?, and Q_2) Is the approach constructive? Is there an algorithm that can enable reconstruction?

3. RECOVERY APPROACH

Simplifying Noisy Measurements. Our starting point is the *modular decomposition property* [7,8] which allows us to write,

$$g(t) = \mathscr{M}_\lambda(g(t)) + \mathscr{R}_g(t), \ t \in [0, \tau) \Longrightarrow \gamma[k] = y[k] + r[k] \tag{4}$$

where $\mathscr{R}_g(t) = \sum_{m \in \mathcal{M}_\lambda} c_m \mathbb{1}_{\mathcal{D}_m}(t)$ is the *residue function*, $\mathbb{1}_{\mathcal{D}}$ is the indicator function on domain $\mathcal{D}$ with $\cup_m \mathbb{1}_{\mathcal{D}_m} = \mathbb{R}$, and $c[m] \in 2\lambda\mathbb{Z}$. Let us define, $\underline{y}[k] \stackrel{\text{def}}{=} (\Delta y)[k] \equiv y[k+1] - y[k]$; Δ denotes the forward-difference operator. Similarly, $\underline{\gamma}[k] = \Delta\gamma[k]$ and $\underline{r} = \Delta\mathscr{R}_\gamma(kT)$. By applying Δ to (4), we obtain,

$$k \in [0, K-2], \ \ \underline{y}[k] = \underline{\gamma}[k] - \sum\nolimits_{m \in \mathcal{M}_\lambda} c_m \delta(kT - t_m) \tag{5}$$

where $\{t_m\} \in (T\mathbb{Z}) \cap [0, \tau)$ are the unknown folding instants—the locations where the modulo non-linearity kicks-in. The triggering rate (density) of t_m depends on the US-ADC threshold (λ). For a given DR, smaller the λ, higher is the folding rate and larger is number of spikes in (5), *i.e.*, $|\mathcal{M}_\lambda| = M$.

When working with noisy samples in (3), we have, $\underline{y_\eta}[k] = \underline{y}[k] + \underline{\eta}[k]$ where $\underline{\eta}[k] = \sum_{s \in \mathcal{S}_d} \mu_s^d \delta\left(kT - t_s^d\right)$ is the sparse signal arising from the action of Δ on η in (3). Given the nature of I/S-N or J/R-N, typically, we do not expect consecutive or boundary samples of $y[k]$ to be corrupted by $\eta[k]$. That is to say, $\{t_s\}$ in (3) are well separated (cf. Fig. 1) and do not occur at locations $t = 0$ or $t = KT$. Excluding such edge cases and "collisions" between η and modulo folding allows us to write $|\mathcal{S}_d| = 2|\mathcal{S}|$. Also, here we do not leverage the relation between t_s^d and t_s. We can now simplify $\underline{y_\eta}$ as,

$$\begin{aligned}\underline{y_\eta}[k] &= \underline{\gamma}[k] - \sum_{m \in \mathcal{M}_\lambda} c_m \delta(kT - t_m) + \sum_{s \in \mathcal{S}_d} \mu_s^d \delta\left(kT - t_s^d\right) \\ &\equiv \underline{\gamma}[k] + \sum\nolimits_{\ell \in \mathcal{L}} q_\ell \delta(kT - t_\ell), \quad \mathcal{L} = \mathcal{M}_\lambda \cup \mathcal{S}_d.\end{aligned} \tag{6}$$

Generally, we expect $|\mathcal{S}| \ll |\mathcal{M}_\lambda|$, *e.g.* eyeballing Fig. 1(b) reveals that $|\mathcal{S}| = 3$ while $|\mathcal{M}_\lambda| > 20$. In essence, given noisy modulo samples, our strategy is to subtract $\{q_\ell, t_\ell\}_{\ell=0}^{L-1}, L = |\mathcal{L}|$ from $\underline{y_\eta}[k]$ resulting in $\underline{\gamma}$. Then, the anti-difference operator Δ^{-1} can be used to obtain $\Delta^{-1}\underline{\gamma}[k] = \gamma[k]$ up to a constant (in the kernel of Δ).

Recovery via Fourier Domain Partitioning. The key to recovering $\underline{\gamma}$ from (6) is that the bandlimited and non-bandlimited parts of $\underline{y_\eta}[k]$ can be partitioned in the Fourier domain. This observation is based on our upcoming paper [10] and a similar principle traces its roots to the work Wolf on *error correction coding* [31], also see [32]. By writing (6) as $\underline{y_\eta} = \underline{\gamma} + \underline{\rho}$, $\underline{\rho}[k] = \sum_{\ell \in \mathcal{L}} q_\ell \delta(kT - t_\ell)$ and denoting the Discrete Fourier Transform (DFT) of $\underline{y}[k]$ by $\widehat{\underline{y}}[n]$, we see that,

$$\widehat{\underline{y}}[n] = \begin{cases} \widehat{\underline{\gamma}}[n] + \widehat{\underline{\rho}}[n] & n \in \mathbb{E}_{P,K-1} \\ \widehat{\underline{\rho}}[n] & n \notin \mathbb{E}_{P,K-1} \end{cases} \tag{7}$$

where, recall that $\mathbb{E}_{P,K} = [0, P] \cup [K-P, K-1]$. We have isolated $\widehat{\underline{\rho}}[n]$ at the Fourier frequencies $n \in [0, K-2] \setminus \mathbb{E}_{P,K-1}$. Note that $\widehat{\underline{\rho}}[n] = \sum_{\ell \in \mathcal{L}} q_\ell \exp\left(-\jmath \frac{\omega_0 n}{T} t_\ell\right), \underline{\omega_0} = 2\pi/(K-1)$ is a parametric curve with $2L$ unknowns, $\{q_\ell, t_\ell\}_{\ell=0}^{L-1}$ where $L = |\mathcal{L}|, \mathcal{L} = \mathcal{M}_\lambda \cup \mathcal{S}_d$. As pointed out by Wolf [31], these $2L$ unknowns can be obtained by curve-fitting using *spectral estimation* methods, in particular by using Prony's method. Algorithmically, once $\{q_\ell, t_\ell\}_{\ell=0}^{L-1}$ are known, we can subtract the contribution of $\underline{\rho}[n]$ from $\underline{y_\eta}$ in (6) thus yielding $\widehat{\underline{\gamma}}[n]$. From this, $\gamma[k]$ is estimated (up to a constant) by applying anti-difference Δ^{-1}. The steps are outlined in Algorithm 1. Note that Algorithm 1 is *agnostic* to λ (unlike the approach in [8]).

Algorithm 1: Exact Recovery from Sparse Outliers

Input: Modulo samples: $\{y[k]\}_{k=0}^{K-1}$, sampling time T, bandwidth Ω, number of folds M and outliers S.
Result: Estimate of HDR samples $\widetilde{\gamma}_{\mathsf{FD}}$.

1) Set $\tau = KT$. Compute $\underline{y} \stackrel{\text{def}}{=} (\Delta y)[k] \equiv y[k+1] - y[k]$.
2) Compute Discrete Fourier Transform (DFT) to obtain $\widehat{\underline{y}}[n]$.
3) Define $z[n] = \widehat{\underline{y}}[n], \ n \in [P+1, K-P-2]$.
4) Apply spectral estimation to $z[n]$ from 3) to obtain estimates $\{\widetilde{q}_\ell, \widetilde{t}_\ell\}_\ell, \ell = 0, \ldots, (M+2S-1)$.
   For further details on this step, see [10].
5) Estimate $\widetilde{\underline{\rho}}[k]$ by plugging $\{\widetilde{q}_\ell, \widetilde{t}_\ell\}_\ell$ (from above) into $\widetilde{\underline{\rho}}[k] = \sum_{\ell \in \mathcal{L}} q_\ell \delta(kT - t_\ell)$.
6) Estimate $\underline{\widetilde{\gamma}_{\mathsf{FD}}}[k] = \underline{y_\eta}[k] - \widetilde{\underline{\rho}}[k], k = 0, \ldots, K-2$.
7) Estimate $\widetilde{\gamma}_{\mathsf{FD}}[k]$ (up to an unknown const.) by applying anti-difference operator Δ^{-1}.
8) Estimate $\widetilde{g}(t)$ by applying sinc-interpolation to $\widetilde{\gamma}_{\mathsf{FD}}[k]$.

Recovery Guarantee. For this approach to work, we need at least $2L$ samples of $\widehat{\underline{\rho}}[n]$. In (7), $\widehat{\underline{\rho}}[n], n \notin \mathbb{E}_{P,K-1}$ which is equivalent to $\widehat{\underline{\rho}}[n], n \in ([0, K-2] \setminus \mathbb{E}_{P,K-1})$. Assuming that $M = |\mathcal{M}_\lambda|$ and $S = |\mathcal{S}|$ are known, $L = M + 2S$. Hence, $|[0, K-2] \setminus \mathbb{E}_{P,K-1}| \geqslant 2L \Rightarrow K - 2P - 2 \geqslant 2(M + 2S)$. Using this with $KT = \tau$ and $P = \lceil \Omega/\omega_0 \rceil$ we obtain the required sampling condition.

$$T \leqslant \frac{\tau}{2\left(M + 2S + \left\lceil \frac{\Omega\tau}{2\pi} \right\rceil + 1\right)}. \tag{8}$$

Algorithm 1 succeeds when the above sampling condition is met. We formally state the result in the following theorem.

Theorem 1 (Modulo Sampling with Sparse Outliers)**.** *Let $g \in \mathcal{B}_\Omega$ be a τ-periodic function. Suppose that we are given K noisy modulo samples $y_\eta[k]$ defined in* (3) *with at most M folds and S outliers. Then, a sufficient condition for recovery of $g(t)$ from $y_\eta[k]$ (up to a constant) is that, $T \leqslant \tau/K$ with $K \geqslant 2\left(M + 2S + \left\lceil \frac{\Omega\tau}{2\pi} \right\rceil + 1\right)$.*

For the the proof, we refer to [10] which uses Algorithm 1, but does not consider the case of I/S-N or J/R-N, *i.e.* $S = 0$.

4. HARDWARE EXPERIMENTS

In numerical simulations, the recovery is exact. Here, we will focus on hardware experiments based on the US-ADC [10]. For a given Ω, we generate $g \in \mathcal{B}_\Omega$ by randomizing (uniform distribution) their Fourier coefficients $\{\widehat{g}_p\}_{|p| \leqslant P = \lceil \Omega/\omega_0 \rceil}$ in (1). We use a digital-to-analog converter (DAC) to map $\gamma[k] = g(kT)$ to $g(t)$. The DAC output is then input to the US-ADC and the modulo signal is sampled via an oscilloscope (DSO-X 3024A). We also acquire the ground truth ($\gamma[k]$) and use the mean-squared error, *i.e.*$\mathcal{E}(\gamma, \widetilde{\gamma}_{\mathsf{FD}}) = \frac{1}{K} \sum_{k=0}^{K-1} |\gamma[k] - \widetilde{\gamma}_{\mathsf{FD}}[k]|^2$ as a quantitive

Table 1: Experimental Parameters for Arbitrary Bandlimited Input in Fig. 5.

n	$T\,(\mu\text{s})$	P	K	$\lvert\mathcal{M}_\lambda^{(n)}\rvert$	$\lvert\mathcal{S}^{(n)}\rvert$	$L^{(n)}$	$\mathcal{E}(\gamma, \widetilde{\gamma}_{\mathsf{FD}})$
1	150	12	334	18	4	26	8.92×10^{-3}
2	150	12	334	19	2	23	1.57×10^{-3}
3	150	12	334	18	2	22	4.30×10^{-4}

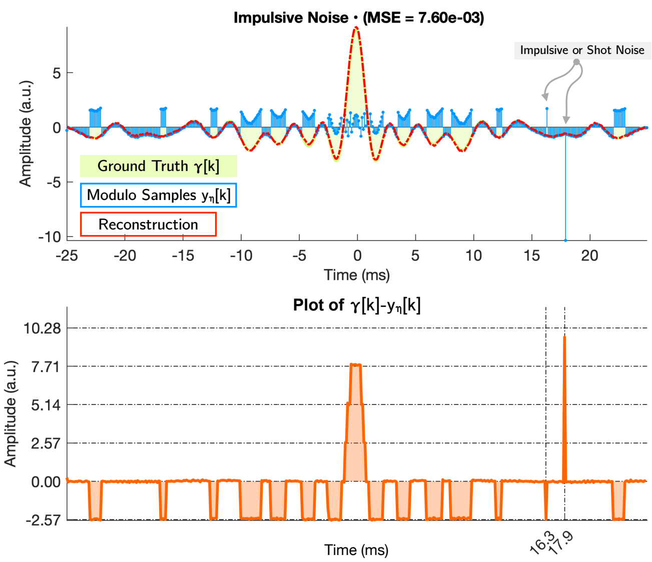

Fig. 3: Hardware Experiment: Recovery with impulsive noise.

performance metric. We use the ground truth to estimate L from the data. The hardware data suffers from additional noise sources, *e.g.* signal quantization and additive Gaussian noise, resulting in $y_\eta[k] = \gamma[k] + \rho[k] + w[k]$ where w is the noise component. To overcome the effects of w and a potentially high value of L, we use the matrix pencil method [33] to stabilize Step 4) of Algorithm 1. The knowledge of L further helps our cause as an effective separation between the signal and noise subspaces is achieved.

Experiment with Impulsive Noise: Fig. 3. The data is shown in Fig. 3(a). In this case, we set $P = 24$ and $\tau = 1/80$ s to generate $g(t)$. We obtain $K = 500$ samples with sampling time $T = 25$ μs. We estimate $|\mathcal{M}_\lambda| = 34$ and as can be seen in Fig. 3(a), $|\mathcal{S}| = 2$. This gives $L = 38$. In Fig. 3(b), we plot $\gamma[k] - y_\eta[k] = -\rho[k]$ (which contains system noise $w[k]$). We can clearly see sparse outliers at $t = 16.3$ s and $t = 17.9$ s. We estimate $\widetilde{\gamma}_{\mathsf{FD}}$ using Algorithm 1 and the MSE is noted to be $\mathcal{E}(\gamma, \widetilde{\gamma}_{\mathsf{FD}}) = 7.6 \times 10^{-3}$.

Experiment with Challenging Noise/Fold Separation: Fig. 4. Let $\mathcal{S}(\tau) = \inf_{0 \leqslant t_\ell, t'_\ell < \tau : t_\ell \neq t'_\ell} |t_\ell - t'_\ell|$ denote the *spike separation*—distance between t_ℓ and t'_ℓ in (6). The presence of I/S-N close to a modulo fold may create algorithmic challenges. This is the case in Fig. 4. With $\{P, \tau, K, T\} = \{12, 0.05\text{s}, 400, 125\mu\text{s}\}$ we generate a different $g \in \mathcal{B}_\Omega$. As seen in the inset of Fig. 4, a modulo fold occurs at $t = 5.875$ ms and the I/S-N is located at $t = 6.375$ ms; this implies $\mathcal{S}(\tau)/T = 3$ samples. Despite the challenge posed by such proximal spikes in (6), Algorithm 1 gracefully reconstructs the signal with MSE $\mathcal{E}(\gamma, \widetilde{\gamma}_{\mathsf{FD}}) = 5.58 \times 10^{-3}$.

Experiment with Jump/Reset Noise: Fig. 5. In this case, we set $P = 12$ and $\tau = 0.05$ s to generate $g(t)$. We obtain $K = 334$ samples with sampling time $T = 150$ μs. We repeat the experiments several times and $n = 1, 2, 3$ such realizations are shown in Fig. 5. The experimental values are tabulated in Table 1. As seen in Fig. 5,

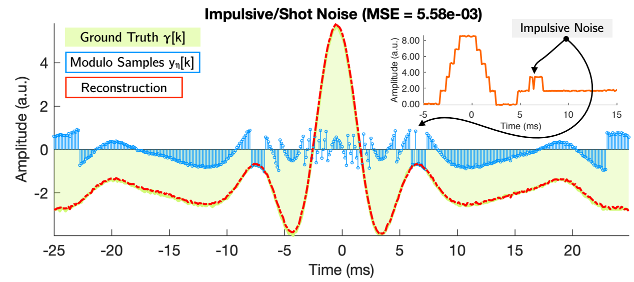

Fig. 4: Hardware Experiment: Recovery when spike-separation between impulsive noise and modulo folding creates an algorithmic challenge. As shown in the inset, the separation distance is $\mathcal{S}(\tau)/T = 3$ samples.

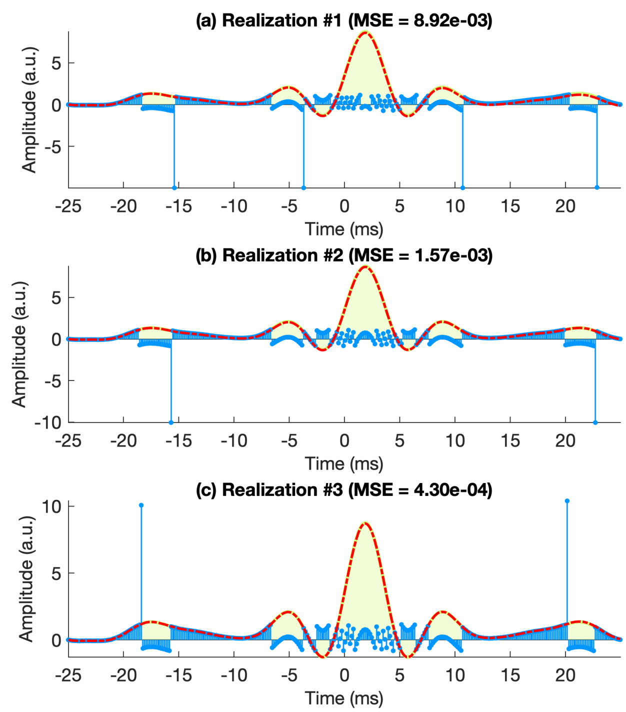

Fig. 5: Hardware Experiment: Recovery with jump/reset noise.

$|\mathcal{S}^{(1)}| = 4$ (top row), $|\mathcal{S}^{(2)}| = 3$ (middle row), $|\mathcal{S}^{(3)}| = 2$ (bottom row), respectively. Since the input signal DR and λ are fixed for the experiment, we get a more-or-less constant value of $|\mathcal{M}_\lambda|$. Despite the system noise, Algorithm 1 offers a competitive performance with the MSE in the range of 10^{-4} to 10^{-3}.

5. CONCLUSION

Hardware implementation of unlimited sampling poses interesting theoretical and practical challenges. In this paper, we studied one such challenge—the problem or signal recovery in presence of sparse outliers. Such outliers arise from impulse noise or due to instabilities of hardware components during signal folding. We showed that sparse outliers can be isolated in the non-bandlimited part of the Fourier spectrum and this allowed us to develop an efficient recovery strategy that is applicable in very realistic scenarios. In presence of other noise sources (*e.g.* Uniform and Gaussian), the promising performance of our method raises interesting questions regarding theoretical recovery guarantees; we plan to cover this aspect in future explorations.

6. REFERENCES

[1] J. Abel and J. Smith, "Restoring a clipped signal," in *IEEE Intl. Conf. on Acoustics, Speech and Sig. Proc. (ICASSP)*, 1991.

[2] T. Olofsson, "Deconvolution and model-based restoration of clipped ultrasonic signals," *IEEE Trans. Instrum. Meas.*, vol. 54, no. 3, pp. 1235–1240, Jun. 2005.

[3] K.-P. Ho, "Maximum-likelihood power estimation for clipped signals," *IEEE Signal Process. Lett.*, vol. 16, no. 7, pp. 569–571, Jul. 2009.

[4] A. Adler, V. Emiya, M. G. Jafari, M. Elad, R. Gribonval, and M. D. Plumbley, "A constrained matching pursuit approach to audio declipping," in *IEEE Intl. Conf. on Acoustics, Speech and Sig. Proc. (ICASSP)*, May 2011.

[5] F. Esqueda, S. Bilbao, and V. Valimaki, "Aliasing reduction in clipped signals," *IEEE Trans. Sig. Proc.*, vol. 64, no. 20, pp. 5255–5267, Oct. 2016.

[6] J. C. Zarnecki and et al., "A soft solid surface on Titan as revealed by the Huygens surface science package," *Nature*, vol. 438, no. 7069, pp. 792–795, Nov. 2005.

[7] A. Bhandari, F. Krahmer, and R. Raskar, "On unlimited sampling," in *Intl. Conf. on Sampling Theory and Applications (SampTA)*, Jul. 2017.

[8] ——, "On unlimited sampling and reconstruction," *IEEE Trans. Sig. Proc.*, vol. 69, pp. 3827–3839, Dec. 2020.

[9] ——, "Methods and apparatus for modulo sampling and recovery," US Patent US10 651 865B2, May, 2020.

[10] A. Bhandari, F. Krahmer, and T. Poskitt, "Unlimited sampling from theory to practice: Fourier-Prony recovery and prototype ADC," *IEEE Trans. Sig. Proc.*, Sep. 2021.

[11] D. Florescu, F. Krahmer, and A. Bhandari, "The surprising benefits of hysteresis in unlimited sampling: Theory, algorithms and experiments," *IEEE Trans. Sig. Proc.*, vol. 70, pp. 616–630, Jan. 2022.

[12] D. Florescu and A. Bhandari, "Unlimited sampling with local averages," in *IEEE Intl. Conf. on Acoustics, Speech and Sig. Proc. (ICASSP) (to appear)*, 2022.

[13] O. Graf, A. Bhandari, and F. Krahmer, "One-bit unlimited sampling," in *IEEE Intl. Conf. on Acoustics, Speech and Signal Processing (ICASSP)*, May 2019, pp. 5102–5106.

[14] D. Florescu, F. Krahmer, and A. Bhandari, "Event-driven modulo sampling," in *IEEE Intl. Conf. on Acoustics, Speech and Sig. Proc. (ICASSP)*, Jun. 2021.

[15] S. Fernandez-Menduina, F. Krahmer, G. Leus, and A. Bhandari, "DoA estimation via unlimited sensing," in *European Sig. Proc. Conf. (EUSIPCO)*, Oct. 2020, pp. 1866–1870.

[16] ——, "Computational array signal processing via modulo non-linearities," *IEEE Trans. Sig. Proc. (in press)*, Jul. 2021.

[17] A. Bhandari, F. Krahmer, and R. Raskar, "Unlimited sampling of sparse signals," in *IEEE Intl. Conf. on Acoustics, Speech and Sig. Proc. (ICASSP)*, Apr. 2018.

[18] ——, "Unlimited sampling of sparse sinusoidal mixtures," in *IEEE Intl. Sym. on Information Theory (ISIT)*, Jun. 2018.

[19] A. Bhandari and F. Krahmer, "HDR imaging from quantization noise," in *IEEE Intl. Conf. on Image Processing (ICIP)*, Oct. 2020, pp. 101–105.

[20] A. Bhandari, M. Beckmann, and F. Krahmer, "The Modulo Radon Transform and its inversion," in *European Sig. Proc. Conf. (EUSIPCO)*, Oct. 2020, pp. 770–774.

[21] M. Beckmann, F. Krahmer, and A. Bhandari, "The modulo radon transform: Theory, algorithms and applications," *SIAM Journal of Imaging Sciences (in press)*, Nov. 2021.

[22] P. Mertz, "Model of impulsive noise for data transmission," *IEEE Trans. Commun.*, vol. 9, no. 2, pp. 130–137, 1961.

[23] J. Rice, "On generalized shot noise," *Advances in Applied Probability*, vol. 9, no. 3, pp. 553–565, Sep. 1977.

[24] M. Zimmermann and K. Dostert, "Analysis and modeling of impulsive noise in broad-band powerline communications," *IEEE Trans. Electromagn. Compat.*, vol. 44, no. 1, pp. 249–258, 2002.

[25] E. Romanov and O. Ordentlich, "Above the Nyquist rate, modulo folding does not hurt," *IEEE Signal Process. Lett.*, vol. 26, no. 8, pp. 1167–1171, Aug. 2019.

[26] O. Musa, P. Jung, and N. Goertz, "Generalized approximate message passing for unlimited sampling of sparse signals," in *IEEE Global Conf. on Sig. and Info. Proc. (GlobalSIP)*. IEEE, Nov. 2018.

[27] M. Cucuringu and H. Tyagi, "On denoising modulo 1 samples of a function," in *Proc. of the* 21^{st} *Intl. Conf. on Artificial Intell. and Stats.*, ser. Proc. of MLR, vol. 84. PMLR, Apr. 2018, pp. 1868–1876.

[28] ——, "Provably robust estimation of modulo 1 samples of a smooth function with applications to phase unwrapping," *Journal of Machine Learning Research*, vol. 21, no. 32, 2020.

[29] S. Rudresh, A. Adiga, B. A. Shenoy, and C. S. Seelamantula, "Wavelet-based reconstruction for unlimited sampling," in *IEEE Intl. Conf. on Acoustics, Speech and Sig. Proc. (ICASSP)*, Apr. 2018.

[30] M. Fanuel and H. Tyagi, "Denoising modulo samples: k-nn regression and tightness of SDP relaxation," May 2021, preprint (arXiv:2009.04850).

[31] J. Wolf, "Redundancy, the discrete Fourier transform, and impulse noise cancellation," *IEEE Trans. Commun.*, vol. 31, no. 3, pp. 458–461, Mar. 1983.

[32] P. Marziliano, M. Vetterli, and T. Blu, "Sampling and exact reconstruction of bandlimited signals with additive shot noise," *IEEE Trans. Inf. Theory*, vol. 52, no. 5, pp. 2230–2233, May 2006.

[33] Y. Hua and T. K. Sarkar, "Matrix pencil method for estimating parameters of exponentially damped/undamped sinusoids in noise," *IEEE Trans. Acoust., Speech, Signal Process.*, vol. 38, no. 5, pp. 814–824, May 1990.